Asymptotics of blowup solutions for the aggregation equation

Yanghong Huang* and Andrea L. Bertozzi†

January 2, 2011

Abstract

We consider the asymptotic behavior of radially symmetric solutions of the aggregation equation $u_t = \nabla \cdot (u \nabla K * u)$ in $\mathbb{R}^n$, for homogeneous potentials $K = |x|^\gamma$, $\gamma > 0$. For $\gamma > 2$, the aggregation happens in infinite time and exhibits a concentration of mass along a collapsing δ-ring. We develop an asymptotic theory for the approach to this singular solution. For $\gamma < 2$, the solution blows up in finite time and we present careful numerics of second type similarity solutions for all γ in this range, including additional asymptotic behavior in the limits $\gamma \to 0^+$ and $\gamma \to 2^-$.

1 Introduction

This paper is devoted to the asymptotic behavior of radially symmetric blowup solutions to the aggregation equation

$$u_t = \nabla \cdot (u \nabla K * u) \quad \text{in } \mathbb{R}^n, \tag{1}$$

where u is the mass density on $\mathbb{R}^n$ and $K * u$ is the convolution of u with some kernel K. This equation arises in a number of models for the self-assembly of nanoparticles [16, 17] and swarming of animal behavior [9, 10, 11, 23, 24, 25]. The mathematical theory of this equation and related generalizations with degenerate or fractional diffusion has also been studied thoroughly in the past few years. The special case in one dimension with degenerate diffusion is investigated by Burger, Capasso, and Morale [10], Burger and Di Francesco [10]. The inviscid case in one dimension is studied theoretically by Bodnar and Velazquez [9] and from an applications point of view in [16, 17], mainly for kernels of the form $K(x) = e^{-|x|}$. Theory for this problem in higher dimensions is studied by Laurent [21] and Bertozzi and Laurent [7] in classical Sobolev spaces, and by Bertozzi and Brandman [4] in L^∞ spaces. Local vs. global well-posedness for this problem is shown to be distinguished by a sharp condition on the kernel [5], namely an Osgood condition involving unboundedness of $\int 1/K'(r)dr$ near the origin. For power-law kernels $K(x) = |x|^\gamma$ this translates into $\gamma = 2$ being the critical power distinguishing finite time vs. infinite blowup. Earlier work by the authors [19] focuses on the special case $\gamma = 1$ for which one finds careful numerical evidence of self-similar blowup behavior in all dimensions. However the blowup involves a self-similar power-law behavior at the blowup time with exponents that do not come from dimensional analysis. The solution remains in some L^p spaces at the blowup time, which motivated the work [8] to study well-posedness in general L^p spaces. The theory for weak measure-valued solutions is developed

*Department of Mathematics, Simon Fraser University, 8888 University Drive Burnaby, British Columbia V5A 1S6, Canada yha82@sfu.ca

†Department of Mathematics, 520 Portola Plaza, University of California, Los Angeles, CA 90095, bertozzi@math.ucla.edu

in [13], based on the underlying gradient flow structure in probability metric space [1] and other techniques from optimal transport [27]. In this context, the discrete system for L particles located at $\{x_1, x_2, \cdots, x_L\}$ with mass $\{m_1, m_2, \cdots, m_L\}$ is a special solution of (1), where the governing ODEs for the particles are

$$\frac{d}{dt}x_i(t) = -\sum_{j\neq i} m_j \nabla K(x_j - x_i), \quad i = 1, 2, \cdots, L. \tag{2}$$

Our work on blowup profiles has inspired new theoretical work [6] on existence of measure solutions for more singular kernels in the case of radially symmetric data. This work proves existence of monotone decreasing measure solutions for power law kernels with $2 - n \leq \gamma < 2$, including the case of the Newtonian potential. It also provides a theoretical framework for which to continue the solution, analyzed in this paper, after the blowup time.

Of particular interest in this equation is the blowup of the smooth or bounded solutions to (1). In one dimension, the same equation with $K(x) = |x|^\gamma/\gamma$, i.e.

$$\frac{\partial u(v,t)}{\partial t} = \frac{\partial}{\partial v}\left[u(v,t)\int_{\mathbb{R}} |v-w|^{\gamma-2}(v-w)u(w,t)dw\right], \tag{3}$$

is well studied as one of the kinetic models in granular flow [26, 3], where $u(v,t)$ is velocity distribution function of the granular medium. The long time asymptotic behavior of the solution is studied first for the special case $\gamma = 3$ in [12] and for general case $\gamma > 1$ in [22].

In this paper, we study various asymptotics of the blowup solutions for the homogeneous kernel $K(x) = |x|^\gamma$ in higher dimensions. The choice of this kernel is for convenience of analysis and similar behaviors are expected for general kernels with leading order $|x|^\gamma$ at the origin. For the special case $\gamma = 2$, thanks to conservation of mass and center of mass, the exact solution can be computed explicitly as

$$u(x,t) = e^{2nMt}u_0(e^{Mt}x), \tag{4}$$

where $u_0(x)$ is the initial condition at time $t = 0$ and $M = \int u(x)dx$ is the total mass of the solution.

When $\gamma \in (2, \infty)$, the solutions exist for any smooth initial data and the only possible blowup is at infinite time [5]. The long time behavior of this blowup process is investigated by introducing a similarity transform, followed by a detailed analysis of the resulting equation in similarity variables in Section 2.

When $\gamma \in (0, 2)$, the solutions exist only on finite time intervals [5]. The dynamics of blowup solutions for the special case $\gamma = 1$ is studied by th authors in [19]. What is interesting about these self-similar blowup solutions is that it has anomalous scaling. In this paper, we show that the same behavior occurs for all $\gamma \in (0, 2)$, in Section 3. We also consider the asymptotic behavior of the solution for $\gamma \to 0^+$ and $\gamma \to 2^-$.

This paper is organized as follows. Section 2 considers the asymptotic form of a radially symmetric blowup for the case $\gamma > 2$. Section 3 considers the blowup profile for the case $0 < \gamma < 2$ showing numerical evidence of a second kind similarly solution in this rage. Section 4 presents some conclusions and open problems.

2 Long time Asymptotics for $\gamma > 2$

The blowup mechanism of the solutions to (1) is ultimately related to the underlying system of ODEs [4] for individual particles. For compactly supported or fast decaying initial data, this

mechanism is determined by the singularity of the kernel at the origin, or the speed of collapse of the underlying particle system (2). For the homogeneous kernel $K(x) = |x|^\gamma$, the larger γ, the slower the speed when two particles collide. This blowup/non-blowup behavior is analyzed rigorously by a generalization of the Osgood condition for ODEs in [5]. In particular, when $\gamma > 2$ the solution blows up only at infinite time. In this section we first examine the long time limit of the solutions after a similarity transformation. Then we consider the special case of a radially symmetric solution for more detailed asymptotics of the infinite time blowup.

2.1 Convergence of general solutions

In this subsection, we will study the long time asymptotics of the solutions to (1). A convenient way to do this is via the *similarity variables*:

$$y = xt^\beta, \quad \tau = \ln t, \quad U = t^{-\alpha} u \tag{5}$$

or $u(x,t) = t^\alpha U(xt^\beta, \tau)$. The new function U satisfies the equation

$$U_\tau = \nabla \cdot [U(\nabla \cdot K * U - \beta y)] \tag{6}$$

provided that

$$\alpha = \frac{n}{\gamma - 2}, \qquad \beta = \frac{1}{\gamma - 2}. \tag{7}$$

These exponents α and β are determined uniquely by the matching condition for the power of t in the equation and the conservation of the mass for U. Such scaling is appropriate for infinite time singularity when $\gamma > 2$ but not for finite time singularity when $\gamma < 2$ as considered later. We note that both the original equation (1) and the transformed equation (6) converses mass, and center of mass (assumed to be at the origin).

The long time behavior of the solution U can be deduced from the associated Lyapunov function, or the energy

$$E(U) = \frac{1}{2} \int_{\mathbb{R}^n} \int_{\mathbb{R}^n} K(y-z) U(y) U(z) dy dz - \frac{\beta}{2} \int_{\mathbb{R}^n} |y|^2 U(x) dx. \tag{8}$$

In fact, the dynamics (6) can be regarded as a gradient flow of this energy in the space of probability measures [27, 1], i.e.

$$\frac{\partial U}{\partial \tau} = -\mathrm{div} \left[U \left(\frac{\delta E}{\delta U} \right) \right] \tag{9}$$

and

$$\frac{d}{d\tau} E(U) = -\int_{\mathbb{R}^n} U(y) |\nabla K * U(y) - \beta y|^2 dx \le 0, \tag{10}$$

where $\frac{\delta E}{\delta U}$ is the Fréchet derivative of the energy E with respect to U.

To include the limiting solution of U, possibly Dirac-delta functions, in the solution space, we introduce the space of measures with center of mass at the origin,

$$\mathcal{M} = \left\{ \mu \text{ is a non-negative Radon measure on } \mathbb{R}^n, \mu(\mathbb{R}^n) = M, \int_{\mathbb{R}^n} y d\mu = 0 \right\}, \tag{11}$$

and the space of probability measures with bounded γ-th order moment

$$\mathcal{P}_\gamma(\mathbb{R}^n) = \left\{ \mu \in \mathcal{M} : \int_{\mathbb{R}^n} |y|^\gamma d\mu < \infty \right\}. \tag{12}$$

By abuse of notation, we write $U(x)dx$ instead of $d\mu$ in the following. For any initial condition $U(\cdot,0) \in \mathcal{P}_\gamma(\mathbb{R}^n)$, we can show that the γ-th order and thus second order moments are bounded uniformly when τ goes to infinity. In fact,

$$\int |y|^2 U(x)dx = \frac{1}{2M}\int (|y|^2 + |z|^2 - 2y\cdot z)U(y)U(z)dydz = \frac{1}{2M}\int\int |y-z|^2 U(y)U(z)dydz \quad (13)$$

Using the Hölder's inequality

$$\int\int |y-z|^2 U(y)U(z)dydz \le \left(\int\int |y-z|^\gamma U(y)U(z)dydz\right)^{2/\gamma} M^{2-4/\gamma}, \quad (14)$$

we have

$$\begin{aligned} E(U) &= \frac{1}{2}\int_{\mathbb{R}^n}\int_{\mathbb{R}^n} |y-z|^\gamma U(y)U(z)dydz - \frac{\beta}{4M}\int\int |y-z|^2 U(y)U(z)dydz \\ &= \frac{1}{2}\left(\int\int |x-y|^2 U(x)U(y)dxdy\right)^{\gamma/2} M^{2-\gamma} - \frac{\beta}{4M}\int\int |x-y|^2 U(x)U(y)dxdy \quad (15) \end{aligned}$$

Since $\gamma > 2$, $E(U)$ is bounded below on $\mathcal{P}_\gamma(\mathbb{R}^n)$ and the second moments (similarly the γ-th order moments) of U are bounded above. Consequently, the boundness of these moments implies the tightness and therefore the weak compactness of the sequence of solutions $U(\tau)$ in $\mathcal{P}_\gamma(\mathbb{R}^n)$. This proves the following theorem:

Theorem 2.1. *Let $U(\tau)$ be the solution to the equation* (6) *in $\mathcal{P}_\gamma(\mathbb{R}^n)$. Then along a subsequence $\{\tau_k\}$, the solutions $\{U(\tau_k)\}$ have a limit in $\mathcal{P}_\gamma(\mathbb{R}^n)$ when τ_k goes to infinity, denoted as U_∞.*

We remark that above argument does not work for the case $\gamma < 2$, in which E is not bounded below. In fact, as first shown numerically in [19] and generalized later in this paper, the self-similar solutions are of the second kind and it is not possible to introduce any exact similarity variables as (5).

Since $E(U)$ is bounded below, from the dissipation inequality (10), any limiting measure U_∞ satisfies the equilibrium condition

$$\int_{\mathbb{R}^n} U_\infty(y)|\nabla K * U_\infty(y) - \beta y|^2 dy = 0. \quad (16)$$

In other words, U_∞ is concentrated on the set where $\nabla K * U_\infty(y) - \beta y$ vanishes. In the community of granular flow, for a given U_∞, the corresponding self-similar solution $u(x,t) = t^\alpha U_\infty(xt^\beta)$ is called a homogeneous cooling state [12]; it is expected to play the same role as the Maxwellian distribution for the Boltzmann equation in rarefied gas dynamics.

However, because the energy $E(U)$ is not convex, the limit U_∞ above can be local minimizers or even saddle points. In general, the convergence of the solution U to the limit is so weak, there is no more information about U_∞ rather than the characterizing equality (16).

2.2 Convergence for radially symmetric solutions

To get more quantative properties about these limiting solutions, we consider only radially symmetric solutions $U_\infty(y) = U_\infty(r)$ in the rest of this section. Denote the characteristic radial velocity, in similarity variables as

$$V(r) = \beta r - \frac{d}{dr} K * U_\infty. \quad (17)$$

Since U_∞ is a non-negative measure, $\frac{d^3}{dr^3}V(r) < 0$ on $(0,\infty)$ and $\frac{d^2}{dr^2}V(0) = 0$. Therefore $\frac{d^2}{dr^2}V(r)$ is concave and $V(r)$ has at most one zero r_0 on $(0,\infty)$, besides the obvious zero at the origin. In other words, from the equilibrium condition (16), U_∞ can only be supported at the origin and r_0. If the fraction of mass concentrated at the origin is λ and the rest on the sphere of radius $r_{0,\lambda}$ is $1-\lambda$, then the limiting solution can be represented as

$$U_{\infty,\lambda}(x) = \lambda M\delta(x) + \frac{(1-\lambda)M}{n\omega_n r_{0,\lambda}^{n-1}}\delta(|x| - r_{0,\lambda}), \tag{18}$$

where ω_n is the volume of the unit sphere in dimension n. Here the radius $r_{0,\lambda}$ of the mass concentrating sphere can be solved from the equation $V(r_{0,\lambda}) = 0$, i.e.

$$r_{0,\lambda} = \left(\frac{1}{\gamma M}\frac{\beta}{\lambda + (1-\lambda)2^{\gamma-1}B(\frac{n+\gamma-1}{2},\frac{n-1}{2})/B(\frac{n-1}{2},\frac{n-1}{2})}\right)^{1/(\gamma-2)}, \tag{19}$$

where B is the Beta function. The corresponding energy is

$$E(U_{\infty,\lambda}) = \frac{(1-\lambda)\beta M r_{0,\lambda}^2}{2\gamma}. \tag{20}$$

We note that the family of limiting solutions $U_{\infty,\lambda}$ for $\lambda > 0$ is unstable: the amount of mass λM concentrated at the origin is exactly that from the initial condition; any perturbation of mass from the origin will expand outward to the mass-concentrating sphere instead of inward to the origin. In fact, $U_{\infty,0}$ corresponds to the global minimizer of the energy (8) in the set of all radially symmetric measures while those $U_{\infty,\lambda}$ with $\lambda \neq 0$ is only a saddle point of the energy. For generic radially symmetric initial data without any concentration of mass at the origin, the solution U converges to the global minimizer $U_{\infty,0}$ (denoted as U_∞ for simplicity). For this reason, we only consider the asymptotic behavior of the solutions to U_∞ in the following and the generalization to the convergence to $U_{\infty,\lambda}$, where $\lambda > 0$ requires only minor modification.

2.3 Asymptotic convergence to the δ-ring for radially symmetric solutions

For smooth initial data $u_0(x)$ decaying fast enough, the solution $u(x,t)$ stays smooth but converges to a δ-ring with vanishing radius when t goes to infinity, as shown in Figure 1 for $\gamma = 4$ in dimension three. The corresponding solution in similarity variables converges to a δ-ring with fixed radius, as shown in Figure 2. The equations (1) and (6) are solved numerically by the method of characteristics. For example, the characteristic equations for the original radial variables are

$$\frac{dr}{dt} = -\frac{\partial}{\partial r}K * u, \quad \frac{du}{dt} = u\Delta_r K * u, \tag{21}$$

where $\Delta_r = \frac{1}{r^{n-1}}\frac{\partial}{\partial r}r^{n-1}\frac{\partial}{\partial r}$ is the Laplacian in the radial variables. The detailed numerical scheme is discussed in the next section when $\gamma \in (0,2)$, in which case much less is known and we have to rely on numerics to guide the analysis.

These figures reveal some non-trivial behavior of the convergence of the solution U towards the δ-ring. This brings the question of the large time, intermediate asymptotics of U. The key observation to derive this refined asymptotics is the fact that the first and second derivatives of the convolution $K*U$ converge to their limiting values much faster, as shown in Figure 3 and 4. In other words, for large τ, the characteristic speed $dr/d\tau$ and the rate of increase of the solution U along

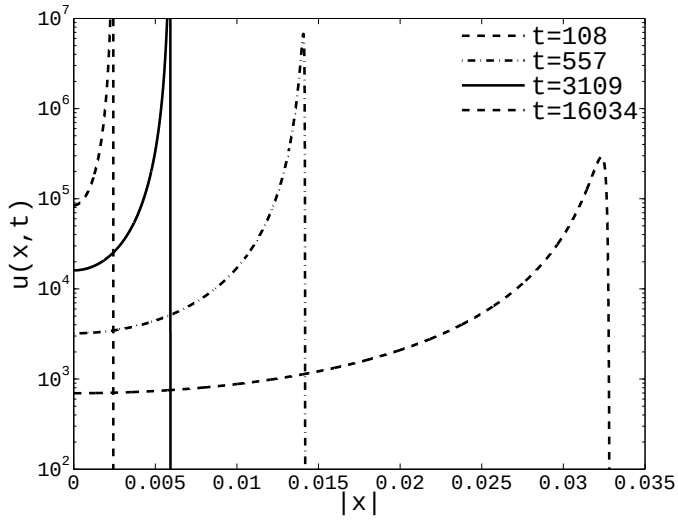

Figure 1: Radially symmetric solution u for the original equation (1) at different times for $\gamma = 4$ in dimension $n = 3$. The solution converges to a δ-ring with vanishing radius.

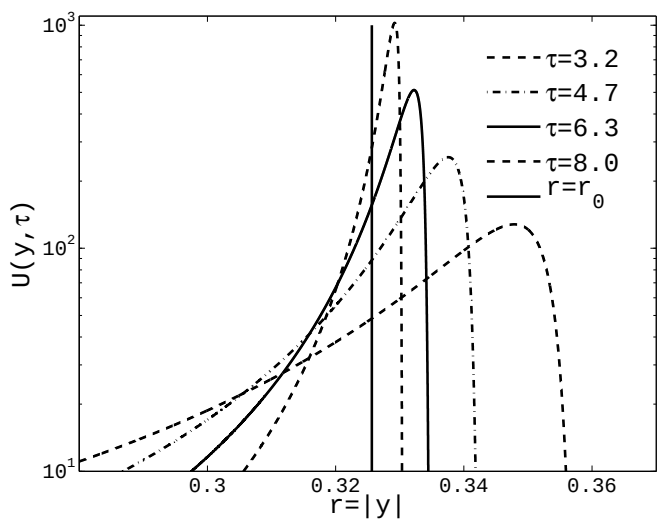

Figure 2: Radially symmetric solution U for the equation (6) in similarity variables at different times for $\gamma = 4$ in dimension $n = 3$. The solution converges to a δ-ring with radius $r_0 \approx 0.325$.

the characteristics become essentially steady. Therefore, the leading order large-time asymptotics for U is governed by the linear first order equation

$$U_\tau = \nabla \cdot [U(\nabla K * U_\infty - \beta y)] \tag{22}$$

in which the convolution $K * U$ is replaced by the effective one $K * U_\infty$. With the radius r_0 of the limiting δ-ring computed from (19) with $\lambda = 1$,

$$r_0 = \left(\frac{\beta}{2^{\gamma-1}\gamma M} \frac{B(\frac{n-1}{2}, \frac{n-1}{2})}{B(\frac{n+\gamma-1}{2}, \frac{n-1}{2})} \right)^{1/(\gamma-2)},$$

the system of ODEs for the characteristic variables r and U of (22) becomes

$$\begin{aligned} \frac{dr}{d\tau} &= \beta r - \frac{M\gamma}{\int_0^\pi \sin^{n-2}\theta d\theta} \int_0^\pi (r - r_0\cos\theta)(r^2 + r_0^2 - 2rr_0\cos\theta)^{\gamma/2-1} \sin^{n-2}\theta d\theta, \\ \frac{dU}{d\tau} &= \left(\frac{M\gamma(n+\gamma-2)}{\int_0^\pi \sin^{n-2}\theta d\theta} \int_0^\pi (r^2 + r_0^2 - 2rr_0\cos\theta)^{\gamma/2-1} \sin^{n-2}\theta d\theta - n\beta \right) U. \end{aligned} \tag{23}$$

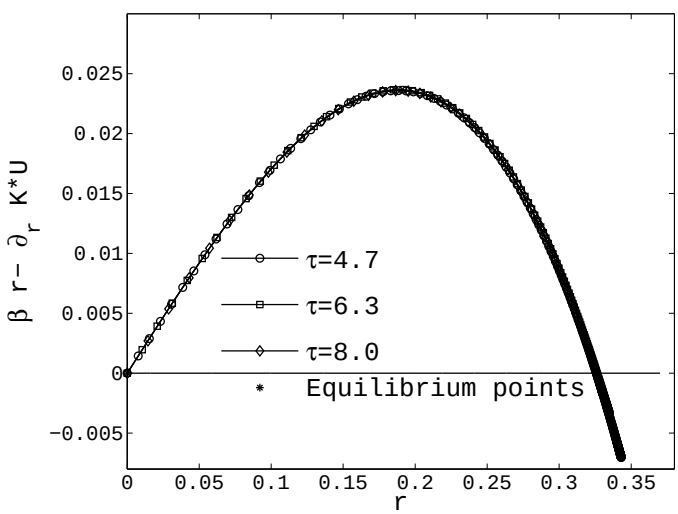

Figure 3: The characteristic velocity $dr/d\tau$ in similarity variables for $\gamma = 4$ in dimension $n = 3$. There are two equilibrium points: the one at the origin is unstable; the one at $r_0 \approx 0.325$ is stable.

For $r < r_0$ near the origin, above characteristic equations can be approximated as

$$\frac{dr}{d\tau} \approx A_0 r, \qquad \frac{dU}{d\tau} \approx (-B_0 + C_0 r^2)U, \tag{24}$$

where

$$A_0 = \beta \left(1 - \frac{\gamma-1}{2^{\gamma-2}} \frac{B(\frac{n-1}{2}, \frac{n-1}{2})}{B(\frac{n+\gamma-1}{2}, \frac{n-1}{2})} \right), \quad B_0 = \beta \left(n - \frac{n+\gamma-2}{2^{\gamma-2}} \frac{B(\frac{n-1}{2}, \frac{n-1}{2})}{B(\frac{n+\gamma-1}{2}, \frac{n-1}{2})} \right),$$
$$C_0 = M(n+\gamma-2)\gamma(\gamma-2)(\gamma-3)r_0^{\gamma-4}.$$

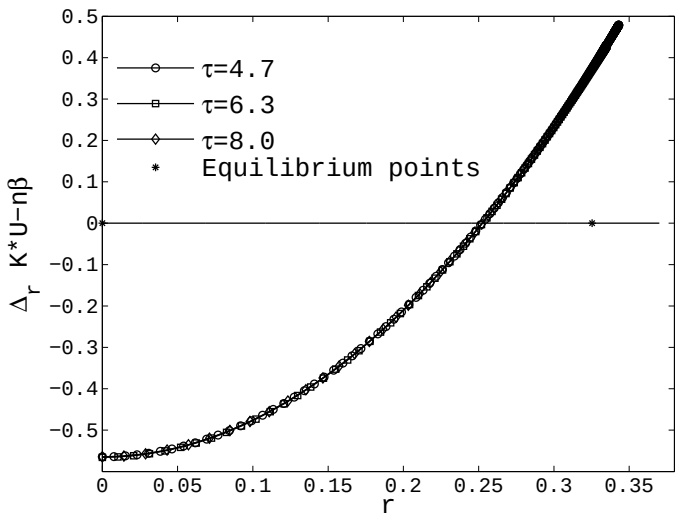

Figure 4: The rate of change of U in similarity variables for $\gamma = 4$ in dimension $n = 3$.

This local approximation leads to the asymptotic solution of the form

$$U(r,\tau) \sim e^{-B_0\tau + \frac{C_0}{2A_0}r^2}, \tag{25}$$

where the prefactor determined by the initial condition is transient and is therefore omitted. The time decay $U(0,\tau) \sim e^{-B_0\tau}$ at the origin is confirmed numerically in Figure 5. The spatial variation of $U(r,\tau) \sim U(0,\tau)e^{C_0 r^2/3}$ near the origin is matched perfectly near the origin in Figure 6; a better matched away from the origin is expected if higher order terms in r are included in (24).

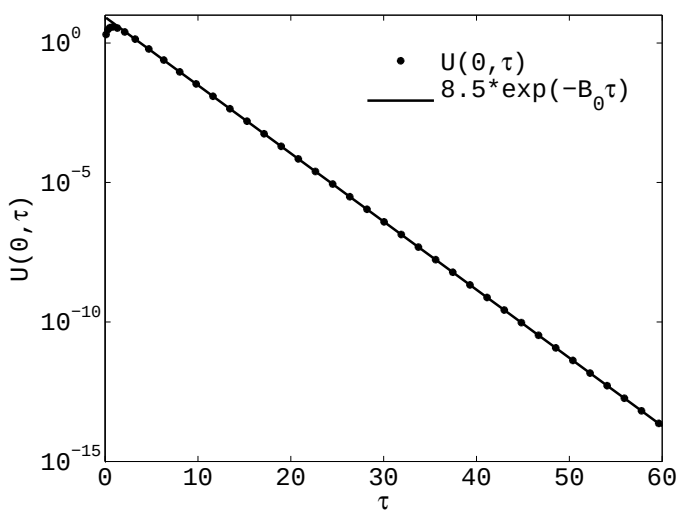

Figure 5: The decay of U at the origin for $\gamma = 4$ in dimension $n = 3$.

For r close to r_0, the characteristic equations can be approximated as

$$\frac{dr}{d\tau} \approx -A_1(r - r_0), \qquad \frac{dU}{d\tau} \approx (B_1 - C_1(r - r_0))U, \tag{26}$$

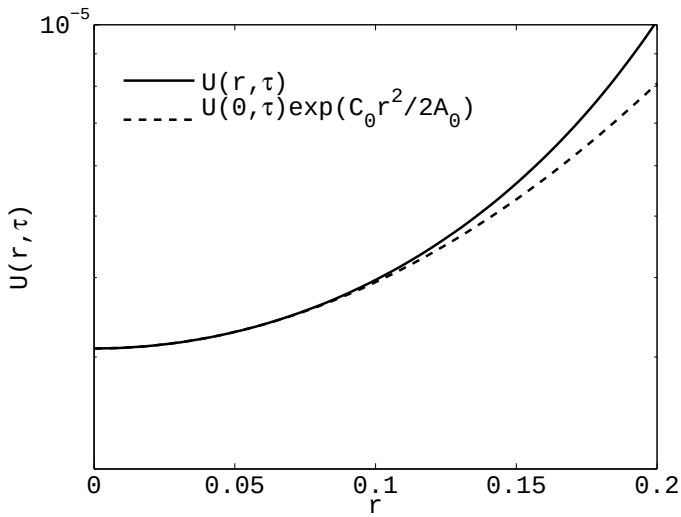

Figure 6: The spatial variation of U near the origin for $\gamma = 4$ in dimension $n = 3$ at $\tau = 8.0$.

where

$$A_1 = (\gamma - 2)\beta, \quad B_1 = (\gamma - 2)\beta, \quad C_1 = \frac{(n + \gamma - 2)\gamma(\gamma - 2)\beta}{2r_0}.$$

This leads to the asymptotic solution of the form

$$U(r, \tau) \sim e^{B_1\tau - C_1 e^{A_1\tau}(r - r_0)/A_1}. \tag{27}$$

However, the prefactor depends strongly on the decay rate of the initial condition, making it useful only at $r = r_0$; the increase rate $O(e^{B_1\tau})$ of U at this point is verified numerically in Figure 7.

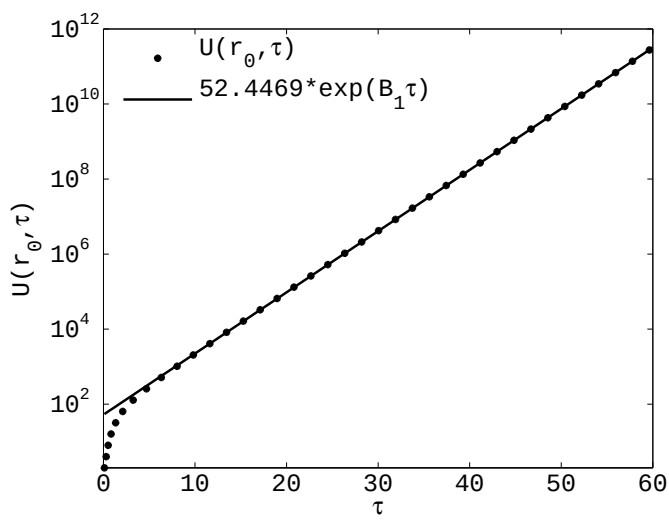

Figure 7: The increase of U at r_0 for $\gamma = 4$ in dimension $n = 3$ at $\tau = 8.0$.

Therefore for generic radially symmetric, smooth initial data, the approach of the solution U to the the limit U_∞ is therefore characterized by the asymptotic scaling (25) and (27). However,

these asymptotic forms do not tell anything about the convergence rate in probability metric like the Wasserstein distances [1]. The convergence in these weaker spaces is in general much more difficult, even for solutions governed by the linearized equation (22).

3 Finite time blowup for $0 < \gamma < 2$

For $\gamma \in (0, 2)$, because of relative strong attraction between particles close enough, smooth solutions blow up in finite time [5]. If T is the blowup time, we can introduce the following similarity variables y and τ,

$$y = x(T-t)^{-\beta}, \quad \tau = -\ln(T-t) \tag{28}$$

and define $U(y, \tau)$ such that

$$u(x,t) = (T-t)^{-\alpha} U(x(T-t)^{-\beta}, \tau), \tag{29}$$

where α and β are unknown constants. Substituting (29) in to the equation for u, the matching condition of the exponents of $(T-t)$ gives the identity

$$\alpha = (n + \gamma - 2)\beta + 1 \tag{30}$$

and the evolution equation

$$U_\tau = \nabla \cdot (U \nabla K * U) - \alpha U - \beta y \cdot \nabla U. \tag{31}$$

If finite mass is concentrated in the core of the blowup profile,

$$\alpha = n\beta \tag{32}$$

must hold for the mass conservation of both u and U. This relation, together with (30), gives the exponents

$$\alpha = \frac{n}{2-\gamma}, \qquad \beta = \frac{1}{2-\gamma}, \tag{33}$$

characterizing self-similar solutions of the *first kind*. Any exact self-similar solutions of this form satisfy the steady equation (31). It is shown in [5] that there are no such exact smooth self-similar solutions in odd dimensions for the special kernel $\gamma = 1$ and in [14] that the only radially symmetric ones are weak measures concentrated at the origin and at most one δ-ring. In fact, for generic radially symmetric, smooth initial data, the solution does not converge to the first-kind self-similar solutions discussed above. In one dimension, the equation with the kernel $\gamma = 1$ can be transformed into Burgers' equation. It is shown in [15] that $\beta = 1.5$ in stead of $\beta = 1$ as from (33) and the corresponding self-similar solutions are of the second kind. It was also recently shown [6] that the multidimensional problem with Newtonian potential $k(x) = |x|^{2-n}$ can be transformed to Burgers equation in the case of radial symmetry. The change of variables gives $\beta = 3/2n$, using the same exact solution of Burgers equation that describes a generic singularity. For more general power-law kernels we must solve the problem numerically, and this is done in general dimension for $\gamma = 1$ by the authors in [19]. The numerics shows a clear second kind similarity solution. The main point of this section is to show that this behavior holds in for all $\gamma \in (0, 2)$.

3.1 Numerical methods and numerical results

The numerical methods is a slight generalization of that in [19] and is reviewed next for completeness. The equation (1) is solved by the method of characteristics, respecting the underlying transport structure of the dynamics. In radial coordinates, the original equation (1) can be written as

$$u_t = \frac{\partial u}{\partial r}\frac{\partial}{\partial r}K * u + u\Delta_r K * u, \tag{34}$$

where $\Delta_r = \partial_{rr} + \frac{n-1}{r}\partial_r$ is the Laplacian in radial variable r. Therefore, the system of ODEs for the characteristics is

$$\frac{dr}{dt} = -\frac{\partial}{\partial r}K * u, \quad \frac{du}{dt} = u\Delta_r K * u, \tag{35}$$

where

$$\partial_r K * u = \gamma c_n \int_0^\infty u(r')r'^{n-1}\int_0^\pi (r - r'\cos\theta)(r^2 + r'^2 - 2rr'\cos\theta)^{\gamma/2-1}\sin^{n-2}\theta d\theta dr', \tag{36a}$$

$$\Delta_r K * u = (n+\gamma-2)\gamma c_n \int_0^\infty u(r')r'^{n-1}\int_0^\pi (r^2 + r'^2 - 2rr'\cos\theta)^{\gamma/2-1}\sin^{n-2}\theta d\theta dr' \tag{36b}$$

and

$$c_n = \pi^{1/2}\Gamma\left(\frac{n-1}{2}\right)/\Gamma\left(\frac{n}{2}\right).$$

The integral in the angular variable θ can be precomputed as a function of r, r' and the ratio r'/r as a consequence of the homogeneity of the kernel. More precisely, we precompute the following integrals

$$\begin{aligned}&\int_0^\pi (r - r'\cos\theta)(r^2 + r'^2 - 2rr'\cos\theta)^{\gamma/2-1}\sin^{n-2}\theta d\theta \\ =&\begin{cases} r^{\gamma-1}\int_0^\pi (1-\rho\cos\theta)(1+\rho^2-2\rho\cos\theta)^{\gamma/2-1}\sin^{n-2}\theta d\theta, \\ (r')^{\gamma-1}\int_0^\pi (\rho-\cos\theta)(1+\rho^2-2\rho\cos\theta)^{\gamma/2-1}\sin^{n-2}\theta d\theta, \end{cases}\end{aligned}$$

$$\int_0^\pi (r^2 + r'^2 - 2rr'\cos\theta)^{\gamma/2-1}\sin^{n-2}\theta d\theta = (\max(r,r'))^{\gamma-2}\int_0^\pi (1+\rho^2-2\rho\cos\theta)^{\gamma/2-1}d\theta$$

where $\rho = \min(r,r')/\max(r,r') \in [0,1]$. With the auxiliary functions

$$I_1(\rho) = \int_0^\pi (1-\rho\cos\theta)(1+\rho^2-2\rho\cos\theta)^{\gamma/2-1}\sin^{n-2}\theta d\theta, \tag{37a}$$

$$I_2(\rho) = \int_0^\pi (\rho-\cos\theta)(1+\rho^2-2\rho\cos\theta)^{\gamma/2-1}\sin^{n-2}\theta d\theta, \tag{37b}$$

$$I_3(\rho) = \int_0^\pi (1+\rho^2-2\rho\cos\theta)^{\gamma/2-1}\sin^{n-2}\theta d\theta, \tag{37c}$$

the complexity is reduced to $O(N^2)$ per time step to evaluate a single integral in r', where N is the number of spatial grid points in the radial coordinate r. Once the characteristic speeds in (35) are found, the system (1) is evolved using classical forth order Runger-Kutta method. The anomalous exponent β and the self-similar profile U can be obtained by post-processing of the solution u [19].

We have shown sample results in the previous section for $\gamma > 2$ and focus on the exponents β and the profiles for $\gamma \in (0,2)$ in the rest for the second-kind self-similar profiles, as shown in Figure 8-12. The profiles are ordered in the far field but not near the origin, if either the dimension n or the power γ is fixed. The anomalous exponents for different γ in different dimensions are shown

in Figure 13. These exponents have a strong dependence on γ but a relative weak dependence on the dimensions. Though there is no explicit formula for these exponents, the asymptotic behavior of β is evident when γ is close to zero or two, both of which are analyzed in the following after some properties of the self-similar profiles are reviewed.

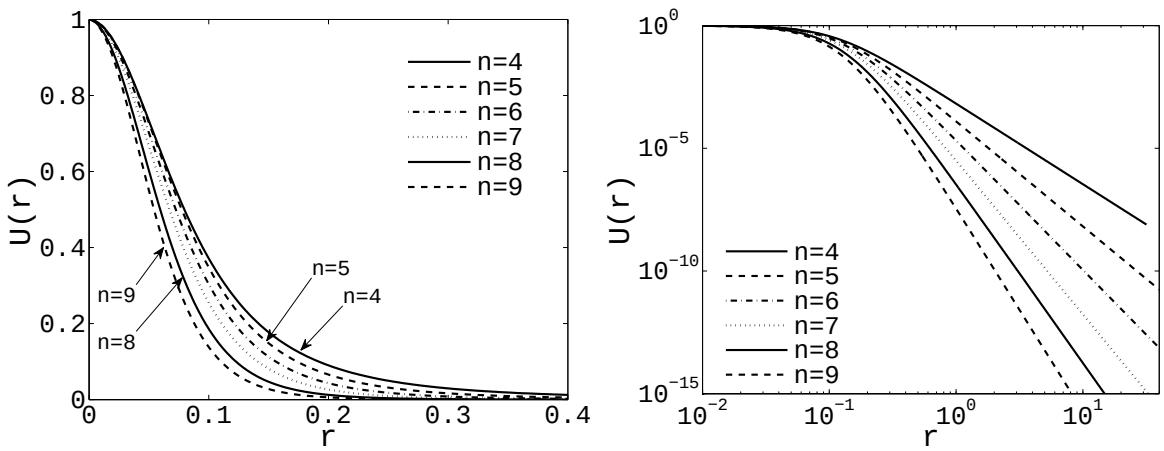

Figure 8: Similarity solution profiles show in the similarity variables U and $r = |y|$ as defined in (28-29), in different space dimensions for $\gamma = 0.4$.

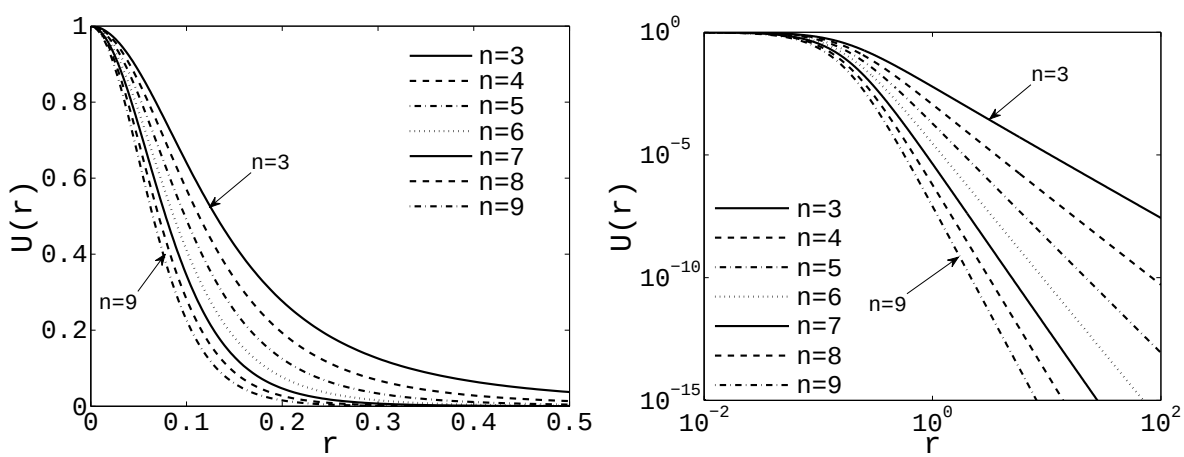

Figure 9: Similarity solution profiles show in the similarity variables U and $r = |y|$ as defined in (28-29), in different space dimensions for $\gamma = 1$.

3.2 Properties of the self-similar profile U

If the self-similar profile U exists, it must satisfy the steady state of (31)

$$\mathcal{A}U = \nabla \cdot (U \nabla K * U) - \alpha U - \beta y \cdot \nabla U = 0, \qquad K(x) = |x|^{\gamma}. \tag{38}$$

A few properties are immediately available. First there is a family of solutions: if U is a solution of (38), so is $U_\lambda(y) = \lambda^{n+\gamma-2} U(\lambda y)$ for any $\lambda > 0$. As a result, all the profiles U shown in Figure 8-12

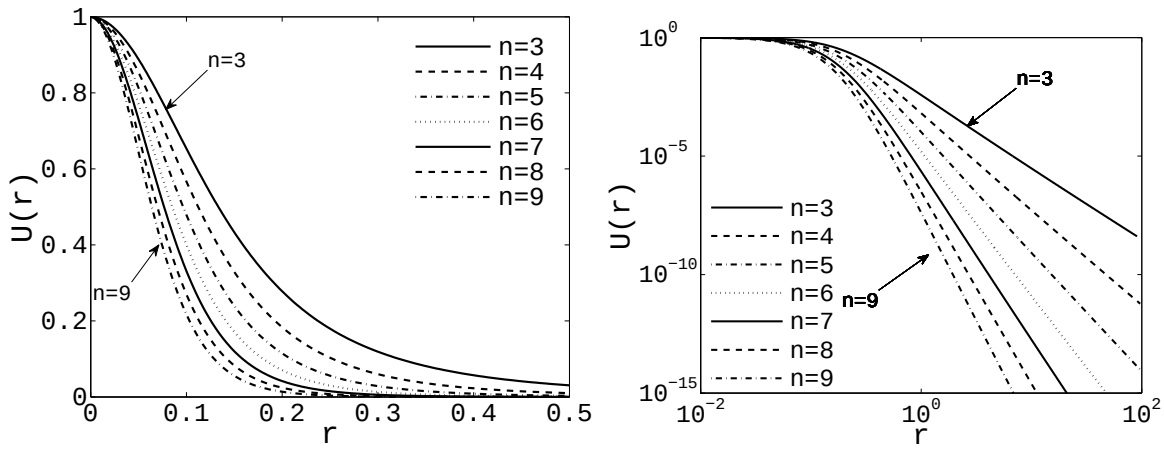

Figure 10: Similarity solution profiles show in the similarity variables U and $r = |y|$ as defined in (28-29), in different space dimensions for $\gamma = 1.6$.

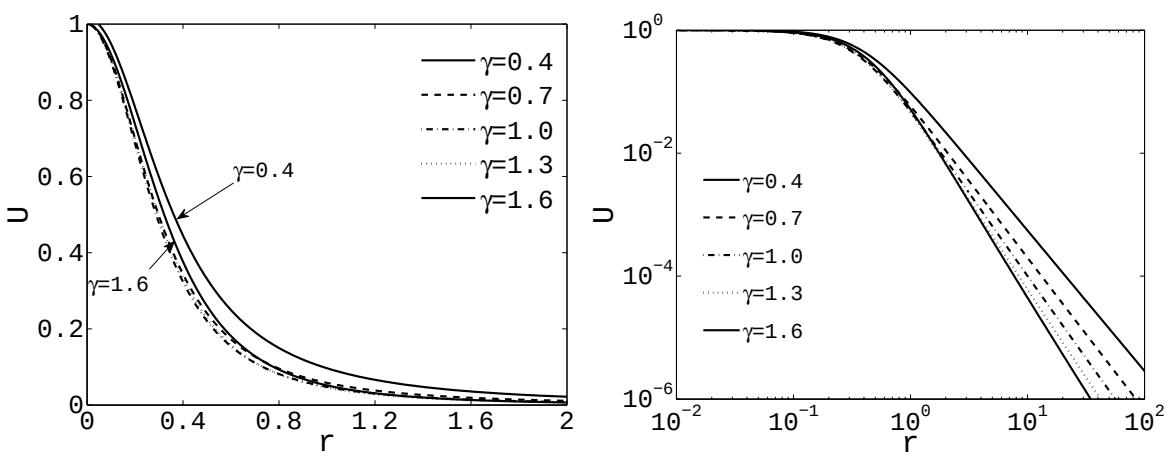

Figure 11: Similarity solution profiles show in the similarity variables U and $r = |y|$, in dimension three for different γ.

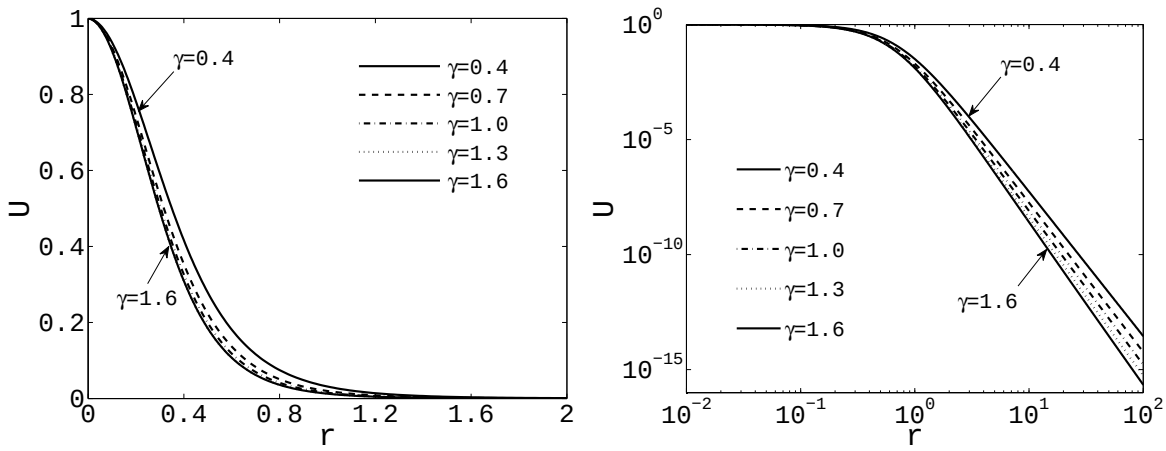

Figure 12: Similarity solution profiles show in the similarity variables U and $r = |y|$, in dimension seven for different γ.

and analyzed below are normalized by the condition $U(0) = 1$. Moreover, this family of solutions gives arise to an eigenpair for the the linearized operator $\mathcal{L}$ at U defined as

$$\mathcal{L}W = \nabla \cdot (U \nabla K * W) + \nabla \cdot (W \nabla K * U) - \alpha W - \beta y \cdot \nabla W. \tag{39}$$

From the invariance of the solution U_λ, we have

$$0 = \frac{d}{d\lambda} \mathcal{A} U_\lambda \bigg|_{\lambda=1} = \mathcal{L} \frac{d}{d\lambda} U_\lambda \bigg|_{\lambda=1} = \mathcal{L}\left[(n+\gamma-2)U + y \cdot \nabla U\right]. \tag{40}$$

This implies that $e_1(y) = (n+\gamma-2)U + y \cdot \nabla U$ is an eigenfunction of $\mathcal{L}$ corresponding to the zero eigenvalue. From this eigenpair and the steady state equation (38), we can get the second eigenpair:

$$\mathcal{L}\left[\alpha U + \beta y \cdot \nabla U\right] = \mathcal{L}(U) = \alpha U + \beta y \cdot \nabla U, \tag{41}$$

or $e_2(y) = \alpha U + \beta y \cdot \nabla U$ is the eigenfunction of $\mathcal{L}$ corresponding to eigenvalue one. This second eigenpair is related to the time translation of the solution $u(x,t) = (T-t)^{-\alpha} U(x(T-t)^{-\beta})$. In other words, if the time t is translated to $t + \epsilon$ or

$$T - t - \epsilon = (T-t)(1 - \epsilon e^\tau) \tag{42}$$

then

$$\begin{aligned} u^\epsilon(x,t) &= (T-t-\epsilon)^{-\alpha} U(x(T-t-\epsilon)^{-\beta}) \\ &= (T-t)^{-\alpha}(1-\epsilon e^\tau)^{-\alpha} U(x(T-t)^{-\beta}(1-\epsilon e^\tau)^{-\beta}) \\ &= u(x,t) + \epsilon e_2(x(T-t)^{-\beta}(1-\epsilon e^\tau)^{-\beta}) + O(\epsilon^2). \end{aligned} \tag{43}$$

Even though this eigenvalue is positive, the blowup profile is stable; any perturbation in this mode results in a translation in blowup time. However, this mode does prevent any direct computation of the profile U from (31), unless the dynamics is restricted on the space orthogonal to e_2.

Another important property is the algebraic decay rate of U in the far field. All the solutions u are observed to collapse into an envelope (Figure 14). This, together with the ansatz (29), implies that $U(y) \sim |y|^{-\alpha/\beta} = |y|^{2-n-\gamma-1/\beta}$ as $|y|$ goes to infinity. This decay rate provides another validation for the numerical results and an equation for the perturbation expansion as γ goes to 2^-.

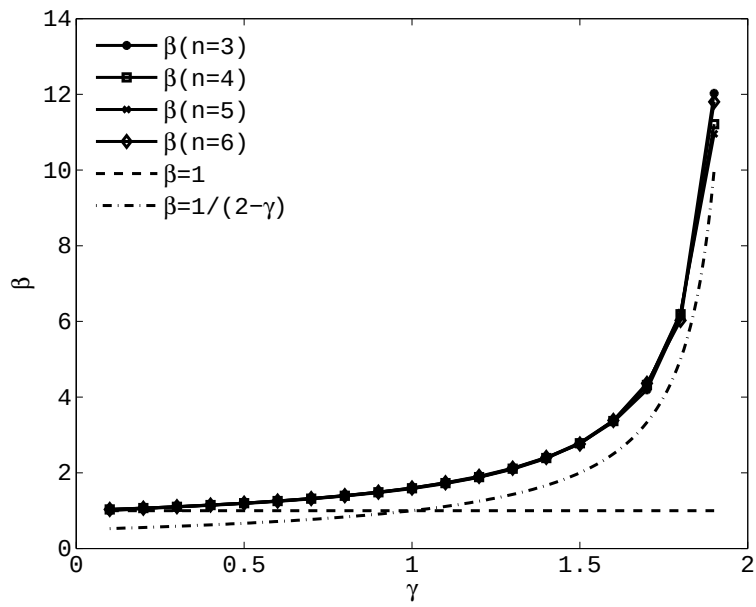

Figure 13: The anomalous exponent β in different dimensions for $\gamma \in (0, 2)$.

3.3 The asymptoics when $\epsilon = \gamma \to 0$

In general, the exponent β in the second-kind self-similar solution is governed by a nonlinear eigenvalue problem [2] and there is no explicit formula as that in the first-kind counterpart. However, for the special case of $K(x) = |x|$ in odd dimension, the exponents are calculated in [20, 18] by transforming the steady state equation (38) into a system of ODEs, followed a shooting method to match the boundary conditions of these two. Furthermore, it is evident from Figure 13 that the exponent β has an asymptotic limit when γ approaches zero and two, which is the subject of this and the next subsection.

When $\epsilon = \gamma$ is close to zero, we first rescale the solution $U_\epsilon(y)$ to $W_\epsilon(y) = U_\epsilon(\epsilon^{1/(n+\epsilon-2)}y)$, since it is W_ϵ instead of U_ϵ that has a well-defined limit when ϵ goes to zero. This rescaling keeps the exponent α_ϵ and β_ϵ invariant and and therefore their asymptotic expansions. More precisely, the equation for W_ϵ is the same as U_ϵ except with the rescaled kernel $\tilde{K}_\epsilon(x) = |x|^\epsilon/\epsilon$, that is

$$\nabla \cdot (W_\epsilon \nabla \tilde{K}_\epsilon * W_\epsilon) = \alpha_\epsilon W_\epsilon + \beta_\epsilon y \cdot \nabla W_\epsilon. \tag{44}$$

The numerical computed β in Figure 13 suggests the following asymptotic expansions for the exponents

$$\beta_\epsilon = 1 + C_1\epsilon + C_2\epsilon^2 + \cdots, \tag{45a}$$

$$\alpha_\epsilon = (n-2+\epsilon)\beta_\epsilon + 1 = n - 1 + ((n-2)C_1 + 1)\epsilon + \cdots, \tag{45b}$$

and for the profile

$$W_\epsilon = W_0 + \epsilon W_1 + \epsilon^2 W_2 + \cdots. \tag{46}$$

Upon substituting them into (44), the resulting leading order $O(1)$ equation is

$$\nabla \cdot (W_0 \nabla \tilde{K}_0 * W_0) = (n-1)W_0 + y \cdot \nabla W_0, \qquad \tilde{K}_0(x) = \ln|x| \tag{47}$$

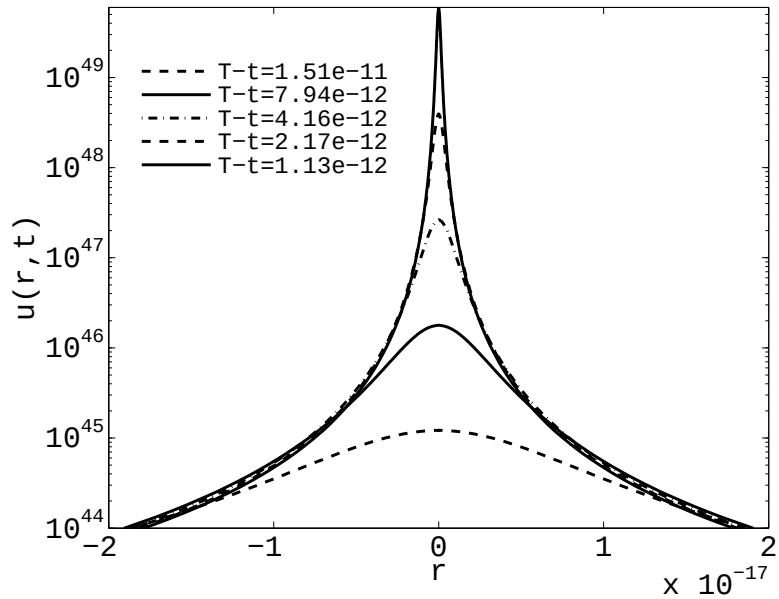

Figure 14: Solution near the blowup time for $\gamma = 1$ in dimension $n = 3$. The solution collapses into envelope $|x|^{-\alpha/\beta}$.

with the boundary conditions

$$W_0(0) = 1, \quad \nabla W_0(y)|_{y=0} = 0, \quad W_0(y) \sim |y|^{1-n} \quad \text{as } |y| \to \infty. \tag{48}$$

Compared with the steady equation (38) for general γ (or ϵ), the integral-differential equation (47) for the limiting profile contains no unknown parameters any more. To get the first order correction for β, we introduce the linearized operator $\mathcal{L}_0$ at W_0

$$\mathcal{L}_0(V) = \nabla \cdot (V \nabla \tilde{K}_0 * W_0) + \nabla \cdot (W_0 \nabla \tilde{K}_0 * V) - (n-1)V - y \cdot \nabla V, \tag{49}$$

and its formal adjoint operator

$$\mathcal{L}_0^*(V) = -\nabla V \cdot \nabla \tilde{K}_0 * W_0 + \nabla \cdot \int_{\mathbb{R}^n} \tilde{K}_0(y-z) W_0(z) \nabla V(z) dz + V + y \cdot \nabla V.$$

It is obvious that from the steady state equation (47),

$$\mathcal{L}_0(W_0) = (n-1)W_0 + y \cdot \nabla W_0 \tag{50}$$

and from the explicit eigenpair (40),

$$\mathcal{L}_0 \left[(n-2)W_0 + y \cdot \nabla W_0 \right] = 0. \tag{51}$$

The $O(\epsilon)$ equation from (44) is

$$\begin{aligned} \mathcal{L}_0(W_1) &= ((n-2)C_1 + 1)W_0 + C_1 y \cdot \nabla W_0 - \nabla \cdot \left[W_0 \left(\frac{y}{|y|^2} \ln |y| \right) * W_0 \right] \\ &= C_1 \mathcal{L}_0(W_0) - C_1 W_0 - \nabla \cdot \left[W_0 \left(\frac{y}{|y|^2} \ln |y| \right) * W_0 \right]. \end{aligned} \tag{52}$$

We can find C_1 from the solvability condition. Since $\mathcal{L}_0$ has a one-dimensional null space, spanned by $(n-2)W_0 + y \cdot \nabla W_0$, the formal adjoint $\mathcal{L}_0^*$ is expected to have a non-trivial null space too, containing a nonzero function W^* such that $\mathcal{L}_0^*(W_0^*) = 0$. The solvability condition for (52) is then obtained by multiplying both sides and integrating on the whole space, i.e.

$$\begin{aligned} 0 &= \int_{\mathbb{R}^n} W_0^* \left(C_1 \mathcal{L}(W_0) - C_1 W_0 - \nabla \cdot \left[W_0 \left(\frac{y}{|y|^2} \ln |y| \right) * W_0 \right] \right) dy \\ &= -C_1 \int_{\mathbb{R}^n} W_0^* W_0 dy - \int_{\mathbb{R}^n} W_0^* \nabla \cdot \left[W_0 \left(\frac{y}{|y|^2} \ln |y| \right) * W_0 \right] dy. \end{aligned} \tag{53}$$

This gives the coefficient C_1 for the first order correction of β a

$$C_1 = -\frac{1}{\int_{\mathbb{R}^n} W_0^* W_0 dy} \int_{\mathbb{R}^n} W_0^* \nabla \cdot \left[W_0 \left(\frac{y}{|y|^2} \ln |y| \right) * W_0 \right] dy. \tag{54}$$

Since both the leading order profile equation (47) and the adjoint equation $\mathcal{L}_0^*(W^*) = 0$ are nonlinear nonlocal, there is no explicit form for the exact solutions and they are also very challenging to be solved numerically. In the special case of even dimensions, we can use the fact that successive Laplacians of the kernel $\tilde{K}_0(y) = \ln |y|$ becomes the fundamental solution of the Laplace equation to compute the convolution $\tilde{K}_0 * W_0$ by a system of ODEs. This observation enables us to transform both integral-differential equations into two systems of ODEs by shooting methods, in the same spirit to calculating the exponent β for the special case $\gamma = 1$ in [20, 18].

We start with dimension $n = 4$, and the case in higher even dimensions can be generalized easily. We introduce the scalar variables $w_0(r)(= W_0(|y|))$, $w_1(r)$, $w_2(r)$ and $w_3(r)$ defined on $[0, \infty)$, such that

$$w_3 = \frac{d}{dr} \tilde{K}_0 * w_0, \quad w_2 = \Delta_r \tilde{K}_0 * w_0, \quad w_1 = w_2',$$

where by abuse of notion, the convolution is alway performed on $\mathbb{R}^n$, but evaluated at $r = |y|$. Upon this change of variables, the governing equation (47) becomes

$$16\pi^2 \left(\frac{dw_0}{dr} w_3 + w_0 w_0 \right) = 3w_0 + r \frac{dw_0}{dr}.$$

Therefore, above system of ODEs can be rewritten as

$$\begin{aligned} \frac{dw_0}{dr} &= -\frac{16\pi^2 w_2 - 3}{16\pi^2 w_3 - r} w_0, \\ \frac{dw_1}{dr} &= -w_0 - \frac{3}{r} w_1, \\ \frac{dw_2}{dr} &= w_1, \\ \frac{dw_3}{dr} &= w_2 - \frac{3}{r} w_3. \end{aligned} \tag{55}$$

This system is equivalent to (47) in the sense that $W_0(y) = w_0(r)$ with $r = |y|$, if the initial conditions at $r = 0$ and far field conditions as r goes to infinity match. The expected decay rate $O(r^{1-n})$ for w_0 implies that both w_1 and w_2 converge to zero as r goes to infinity and shooting method is used to choose $w_i(0)$s appropriately to enforce these decay conditions in the far field. The dimension $n = 4$ is special because these initial conditions are determined completely by the local well-posedness of the system (55), i.e

$$w_1(0) = 0, \quad w_2(0) = 3/16\pi^2, \quad w_3(0) = 0.$$

and $w_0(0) = 1$ for normalization. To avoid the singularity at the origin, the system (55) is be solved with any ODE solver starting at small $r > 0$, where the solution can be represented as a rapidly converging power series.

Once the profile $w_0(= W_0)$ is found, the solution (or the eigenfunction) to the adjoint equation $\mathcal{L}_0^*(W_0^*) = 0$ is obtained similarly. Let $w_0^* = W_0^*$ and $\frac{d}{dr}w_1^* = W_0 \frac{y}{|y|} \cdot \nabla W_0^*$, then the second term in $\mathcal{L}_0^*(W_0^*)$ can rewritten as

$$\nabla \cdot \int_{\mathbb{R}^n} \nabla w_1^*(y) \ln|x-y| dy = -\nabla \cdot \int_{\mathbb{R}^n} w_1^*(y) \nabla_y \ln|x-y| dy = \Delta_r \ln|x| * w_1^*. \tag{56}$$

Denote the last convolution integral $\Delta_r \ln|x| * w_1^*$ as w_3^* and let $w_2^* = \frac{d}{dr}w_3^*$, then the system of ODEs for the variables associated with the adjoint equation becomes

$$\begin{aligned}
\frac{dw_0^*}{dr} &= -\frac{16\pi^2 w_2^* + w_0^*}{16\pi^2 w_3^* - r}, \\
\frac{dw_1^*}{dr} &= -\frac{16\pi^2 w_2^* + w_0^*}{16\pi^2 w_3^* - r} w_0, \\
\frac{dw_2^*}{dr} &= -w_1^* - \frac{3}{r} w_2^*, \\
\frac{dw_3^*}{dr} &= w_2^*.
\end{aligned} \tag{57}$$

The initial condition $w_0^*(0) = 1$ is chosen for normalization in the one-dimensional family of solutions. By the local well-posedness of above system and the even symmetry of w_1^* and w_3^*, we must have $w_2^*(0) = -w_0^*(0) = -1/16\pi^2$ and $w_2^*(0) = 0$. This leaves the problem of finding the shooting parameter $w_3^*(0)$ such that $w_0(r)$ goes to zero as r goes to infinity. Once both the profile w_0 and the solution w_0^* to the adjoint equation are found, the coefficient in the first order correction of β can be evaluated from (54). The comparison of this correction with the numerically computed β is shown in Figure 15, where C_1 estimated from (54) is approximately 2.17 in dimension four. In higher dimensions, the two systems of ODEs (55) and (57) can be solved similarly, with more shooting parameters (or initial conditions) and therefore more difficult to solve [20].

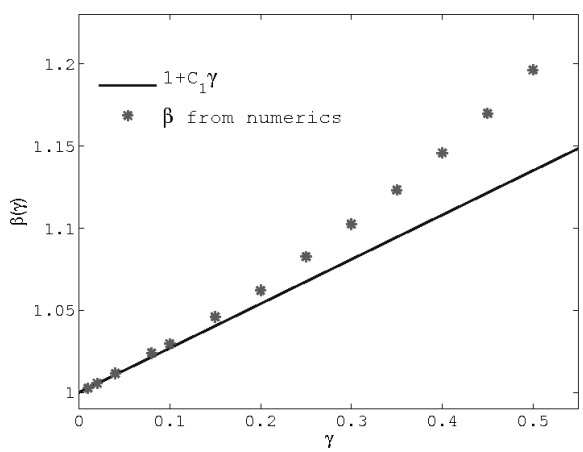

Figure 15: The comparison of the first order correction and the numerically computed β in dimension four. Here C_1 estimated from (54) is approximately 2.17.

3.4 The asymptotics when $\epsilon = 2 - \gamma \to 0$

When $\gamma \to 2$, the asymptotic form suggested from Figure 13 is

$$\beta_\epsilon = \frac{C_0}{\epsilon} + C_1 + C_2\epsilon + \cdots , \tag{58a}$$

$$\alpha_\epsilon = (2-\epsilon)\beta_\epsilon + 1 = \frac{nC_0}{\epsilon} + (nC_1 - C_0 + 1) + \cdots . \tag{58b}$$

Unlike the previous case when $\gamma \to 0$, because of the relative slow decay of the integrand in the convolution, two asymptotic expansions

$$U_\epsilon = U_0 + \epsilon U_1 + \epsilon^2 U_2 + \cdots \tag{59a}$$

and

$$U_\epsilon = \tilde{U}_\epsilon(1 + \epsilon W_1 + \epsilon^2 W_2 + \cdots) \tag{59b}$$

are employed, where

$$\begin{aligned}\tilde{U}_\epsilon &= [U_0]^{1+\epsilon v_1 + \epsilon^2 v_2 + \cdots} \\ &= U_0\left[1 + \epsilon v_1 \ln U_0 + \epsilon^2\left(v_2 \ln U_0 + \frac{1}{2}v_1^2 \ln^2 U_0\right) + \cdots\right]\end{aligned} \tag{60}$$

for some constants v_1,v_2,$\cdots$. The first one (59a) is uniform when $|y|$ is close to the origin while the second one (59b) is uniform when $|y|$ is large and is the one that has to be used in the convolution. Here $\tilde{U}_\epsilon$ characterizes the power decay of the solution U_ϵ and W_is changes slower than any power at infinity. These two asymptotic expansions are related, for example

$$U_1 = U_0(W_1 + v_1 \ln U_0).$$

The non-uniformity of the first one (59a) is obvious, because of the factor $\ln U_0$ in U_1 for any $v_1 \neq 0$.

The constants v_1, v_2, $\cdots$, can be calculated from the relation between the expected leading order decay of $U_0(y) \sim |y|^{-n}$ and that of $U_\epsilon(x) \sim |y|^{-\alpha_\epsilon/\beta_\epsilon}$, i.e.

$$n(1 + \epsilon v_1 + \epsilon^2 v_2 + \cdots) = \frac{\alpha_\epsilon}{\beta_\epsilon} = n - \epsilon + \frac{1}{\beta_\epsilon}, \tag{61}$$

which gives

$$v_1 = \frac{1}{n}\left(\frac{1}{C_0} - 1\right), \quad v_2 = -\frac{C_1}{nC_0^2}, \quad \cdots . \tag{62}$$

For bounded y, using (59a), the right hand side of the steady state

$$\nabla \cdot (U_\epsilon \nabla |y|^{2-\epsilon} * U_\epsilon) = \alpha_\epsilon U_\epsilon + \beta_\epsilon y \cdot \nabla U_\epsilon \tag{63}$$

becomes

$$\begin{aligned}&\frac{C_0}{\epsilon}\nabla \cdot (yU_0(y)) + [C_1 \nabla \cdot (yU_0(y)) + C_0 \nabla \cdot (yU_1(y)) + (1 - C_0)U_0(y)) \\ &+ \epsilon[C_2 \nabla \cdot (yU_0(y)) + C_1 \nabla \cdot (yU_1(y)) + C_0 \nabla \cdot (yU_2(y)) + (1 - C_0)U_1 - C_1 U_0] + \cdots\end{aligned} \tag{64}$$

The left hand of the steady state (63) can be written as

$$\begin{aligned}&U_\epsilon(y)\int_{\mathbb{R}^n} \Delta K(y - y')U_\epsilon(y')dy' + \nabla U_\epsilon(y) \cdot \int_{\mathbb{R}^n} \nabla K(y - y')U_\epsilon(y')dy' \\ &= (2n - (n+2)\epsilon + \epsilon^2)U_\epsilon(y)\int_{\mathbb{R}^n} |y - y'|^{-\epsilon} U_\epsilon(y')dy' + (2 - \epsilon)\nabla U_\epsilon(y) \cdot \int_{\mathbb{R}^n} (y - y')|y - y'|^{-\epsilon} U_\epsilon(y')dy'\end{aligned} \tag{65}$$

We are going to use the expansion (59a) for $U_\epsilon(y)$ and (59b) for $U_\epsilon(y')$ in above expression, where the $O(\epsilon^{-1})$ constant term comes from the convolution integrals for the slow algebraic decay of the integrand. When $|y'|$ is large, $|y-y'|^{-\epsilon}$ can be expanded as

$$\begin{aligned}|y-y'|^{-\epsilon} &= |y'|^{-\epsilon}\exp\left(-\epsilon\ln\frac{|y-y'|}{|y'|}\right)\\ &= |y'|^{-\epsilon}\left[1-\epsilon\ln\frac{|y-y'|}{|y'|}+\frac{\epsilon^2}{2}\ln^2\frac{|y-y'|}{|y'|}+\cdots\right]\end{aligned} \tag{66}$$

The non-uniformity when $|y-y'|$ is small turns to be unimportant since the associated integrals are absolutely integrable.

To further facilitate the calculation, we assume the following asymptotic form of the integrals

$$\int_{\mathbb{R}^n}|y'|^{-\epsilon}\tilde{U}_\epsilon(y')dy' = \frac{A_0}{\epsilon}+A_1+\epsilon A_2+\cdots, \tag{67a}$$

$$\int_{\mathbb{R}^n}|y'|^{-\epsilon}\tilde{U}_\epsilon(y')W_1(y')dy' = \frac{B_0}{\epsilon}+B_1+\epsilon B_2+\cdots, \tag{67b}$$

$$\int_{\mathbb{R}^n}|y'|^{-\epsilon}\tilde{U}_\epsilon(y')W_2(y')dy' = \frac{D_0}{\epsilon}+D_1+\epsilon D_2+\cdots. \tag{67c}$$

The exact values of these constants A_i, B_i and D_i are not used, as we show later.

With all the expansions above, keeping all terms up to $O(\epsilon)$, the first term in (65) can be simplified as

$$\begin{aligned}&(2n-(n+2)\epsilon+\epsilon^2)(U_0(y)+\epsilon U_1(y)+\cdots)\int_{\mathbb{R}^n}|y-y'|^{-\epsilon}\tilde{U}_\epsilon(y')(1+\epsilon W_1(y')+\cdots)dy'\\ &= 2nU_0(y)\int_{\mathbb{R}^n}|y'|^{-\epsilon}\left(1+\epsilon W_1(y')+\epsilon^2W_2(y')\right)\tilde{U}_\epsilon(y')dy'\\ &\quad+\epsilon(2nU_1(y)-(n+2)U_0(y))\int_{\mathbb{R}^n}(1+\epsilon W_1(y'))\tilde{U}_\epsilon(y')dy'\\ &\quad+\epsilon(2nU_2(y)-(n+2)U_1(y)+U_0(y))\int_{\mathbb{R}^n}|y'|^{-\epsilon}\tilde{U}_\epsilon(y')dy'\\ &\quad-2\epsilon nU_0(y)\int_{\mathbb{R}^n}|y'|^{-\epsilon}\tilde{U}_\epsilon(y')\ln\frac{|y-y'|}{|y'|}dy'+O(\epsilon^2)\\ &= 2nU_0(y)(\frac{A_0}{\epsilon}+(A_1+B_0)+\epsilon(A_2+B_1+D_0))\\ &\quad+(2nU_1(y)-(n+2)U_0(y))(A_0+\epsilon(A_1+B_0))+\epsilon(2nU_2(y)-(n+2)U_1(y)+U_0(y))A_0\\ &\quad-2\epsilon nU_0(y)\int_{\mathbb{R}^n}U_0(y')\ln\frac{|y-y'|}{|y'|}dy'+O(\epsilon^2)\end{aligned} \tag{68}$$

and the second term in (65)

$$\begin{aligned}&(2-\epsilon)(\nabla U_0(y)+\epsilon\nabla U_1(y)+\cdots)\int_{\mathbb{R}^n}(y-y')|y-y'|^{-\epsilon}\tilde{U}_\epsilon(y')(1+\epsilon W_1(y')+\cdots)dy'\\ &= 2y\cdot\nabla U_0(y)(\frac{A_0}{\epsilon}+(A_1+B_0-\frac{A_0}{n})+\epsilon(A_2+B_1+D_0-\frac{A_1}{n}-\frac{B_0}{n}))\end{aligned} \tag{69}$$

$$\begin{aligned}&+x\cdot\nabla(2U_1(y)-U_0(y))(A_0+\epsilon(A_1+B_0+\frac{A_0}{n}))\\ &-2\epsilon y\cdot\nabla U_0(y)\int_{\mathbb{R}^n}U_0(y')\ln\frac{|y-y'|}{|y'|}dy'+2\epsilon\nabla U_0(y)\cdot\int_{\mathbb{R}^n}y'U_0(y')\left(\ln\frac{|y-y'|}{|y'|}+\frac{y\cdot y'}{|y'|^2}\right)dy'\end{aligned} \tag{70}$$

Therefore, the leading order $O(\frac{1}{\epsilon})$ equation of (63) is

$$2A_0\nabla\cdot(yU_0(y)) = C_0\nabla\cdot(yU_0(y)) \tag{71}$$

which gives $C_0 = 2A_0$.

The $O(1)$ equation is

$$\left(2A_1 + 2B_0 - \frac{n+2}{n}A_0 - C_1\right)\nabla\cdot(yU_0(y)) + (C_0 - 1)U_0(y) = 0 \tag{72}$$

There exists a non-trivial solution $U_0(y)$ satisfying the boundary condition $U_0(0) = 1$ and $U_0(y) \sim |y|^{-n}$ only when both coefficients vanish, i.e

$$C_0 = 1, \quad 2A_1 + 2B_0 - C_1 = \frac{n+2}{2n}. \tag{73}$$

Finally the $O(\epsilon)$ order equation is

$$\begin{aligned} &C_1U_0(y) + \left(2A_2 + 2B_1 + 2D_0 - \frac{n+2}{n}(A_1 + B_0) - C_1\right)\nabla\cdot(yU_0(y)) \\ &= 2\nabla\cdot(yU_0(y))\int_{\mathbb{R}^n} U_0(y')\ln\frac{|y-y'|}{|y'|}dy' - 2\nabla U_0(y)\cdot\int_{\mathbb{R}^n} y'U_0(y')\left(\ln\frac{|y-y'|}{|y'|} + \frac{(y,y')}{|y'|^2}\right)dy' \end{aligned} \tag{74}$$

Evaluating above equation at $y = 0$, we can get

$$n\left(2A_2 + 2B_1 + 2D_0 - \frac{n+2}{n}(A_1 + B_0) - C_1\right) + C_1 = 0 \tag{75}$$

As a result, the governing equation (74) can be simplified as

$$\begin{aligned} \frac{C_1}{n}y\cdot\nabla U_0(y) = 2\nabla U_0(y)\cdot\int_{\mathbb{R}^n} y'U_0(y')\left(\ln\frac{|y-y'|}{|y'|} + \frac{y\cdot y'}{|y'|^2}\right)dy' \\ -2\nabla\cdot(yU_0(y))\int_{\mathbb{R}^n} U_0(y')\ln\frac{|y-y'|}{|y'|}dy' \end{aligned} \tag{76}$$

The unknown constant C_1 can be determined from the self-consistent condition of above equation when $|x|$ goes to infinity. Since the $U_0(y)$ decays like $O(|y|^{-n})$, so is the left hand side of (76). The second term on the right hand side decays faster than $O(|y|^{-n})$ only the leading order $O(|y|^{-n})$ balances the left hand. In other words, the constant C_1 satisfies the condition

$$C_1 = \lim_{|y|\to\infty}\frac{2}{|y|^2}\int_{\mathbb{R}^n} y\cdot y'U_0(y')\left(\ln\frac{|y-y'|}{|y'|} + \frac{y\cdot y'}{|y'|^2}\right)dy'. \tag{77}$$

In general, this limit can be dominated by the behavior of U_0 near the origin or in the far field. Even though C_1 is known explicitly, there is no simple way to solve the governing equation (76) like the shooting method of the equivalent system of ODEs discussed in previous section. However, the coefficient C_1 can be estimated from (77) for any numerically calculated profile U_0 when γ is close to two. The comparison of the numerical computed β and its first order asymptotic expansion is shown in Figure 16, where $C_1(\approx 1.42)$ is estimated from (77) with the limiting profile U_0 calculated with $\gamma = 1.98$ and the limit taken at $|y| = 10^5$.

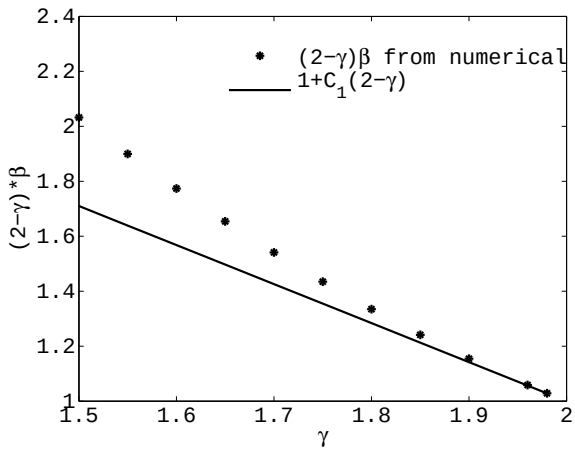

Figure 16: The comparison of the first order correction and the numerically computed β (rescaled by $2-\gamma$) in dimension four. Here $C_1(\approx 1.42)$ is estimated from (77) with the limiting profile U_0 calculated with $\gamma = 1.98$ and the limit taken at $|y| = 10^5$.

4 Conclusion

We have analyzed the asymptotic behavior of two types of blowup solutions to the aggregation equation $u_t = \nabla \cdot (u \nabla K * u)$, depending on the power of the homogeneous kernel $K(x) = |x|^\gamma$. The phenomena when $\gamma > 2$ is studied thoroughly for the one-dimensional granular flow [26, 3], but the anomalous scaling in the self-similar solutions are studied only recently in [19]. This paper gives a complete picture of the generic radially symmetric blowup solutions for this simple kernel, whose analysis is guided heavily by numerical simulations, especially the asymptotic behavior of the anomalous exponent when γ is close to zero and two. However, the stability of these solutions under non-radial perturbation and the possibility of other (stable or unstable) self-similar solutions remains unknown and is challenging numerically too. Another important generalization is the introduction of additional smoothing effects, like degenerate or fractional diffusion. This may lead to more physical steady state solutions instead of the singular ones considered here. We also note that the recent work [6] proves existence of blowup solutions that can be continued for all time as measures, in the case of radially symmetric monotone decreasing data for $2 - n \leq \gamma < 2$. The monotonicity property is preserved for this range of γ, a feature observed in our numerical simulations but not proved rigorously until this new work. It would be interesting to examine the initial blowup profile for these more singular kernels in the range $2 - n < \gamma < 0$ for which no numerical results currently exist.

Acknowledgments

The majority of this work was carried out as part of the PhD thesis [18] of the first author under the direction of the second author. The research was supported by NSF grant DMS-0907931.

References

[1] Luigi Ambrosio, Nicola Gigli, and Giuseppe Savaré. *Gradient flows in metric spaces and in the space of probability measures*. Lectures in Mathematics ETH Zürich. Birkhäuser Verlag, Basel, second edition, 2008.

[2] D. G. Aronson and J. L. Vázquez. Anomalous exponents in nonlinear diffusion. *J. Nonlinear Sci.*, 5(1):29–56, 1995.

[3] D. Benedetto, E. Caglioti, and M. Pulvirenti. A kinetic equation for granular media. *RAIRO Modél. Math. Anal. Numér.*, 31(5):615–641, 1997.

[4] A. L. Bertozzi and J. Brandman. Finite-time blow-up of L^∞-weak solutions of an aggregation equation. *Commun. Math. Sci.*, 8(1):45–65, 2010.

[5] A. L. Bertozzi, J. A. Carrillo, and T. Laurent. Blow-up in multidimensional aggregation equations with mildly singular interaction kernels. *Nonlinearity*, 22(3):683–710, 2009.

[6] A. L. Bertozzi, J. B. Garnett, and T. Laurent. Characterization of radially symmetric finite time blowup in multidimensional aggregation equations, 2011.

[7] A. L. Bertozzi and T. Laurent. Finite-time blow-up of solutions of an aggregation equation in $\mathbf{R}^n$. *Comm. Math. Phys.*, 274(3):717–735, 2007.

[8] A. L. Bertozzi, T. Laurent, and J. Rosado. L^p theory for the multidimensional aggregation equation. *Comm. Pur. Appl. Math.*, 64(1):45–83, 2011.

[9] M. Bodnar and J. J. L. Velazquez. An integro-differential equation arising as a limit of individual cell-based models. *J. Differential Equations*, 222(2):341–380, 2006.

[10] M. Burger, V. Capasso, and D. Morale. On an aggregation model with long and short range interactions. *Nonlinear Anal. Real World Appl.*, 8(3):939–958, 2007.

[11] Martin Burger and Marco Di Francesco. Large time behavior of nonlocal aggregation models with nonlinear diffusion. *Networks and Heterogeneous Media (NHM)*, 3(4):749 – 785, 2008.

[12] E. Caglioti and C. Villani. Homogeneous cooling states are not always good approximations to granular flows. *Arch. Ration. Mech. Anal.*, 163(4):329–343, 2002.

[13] J. A. Carrillo, M. DiFrancesco, A. Figalli, T. Laurent, and D. Slepcev. Global-in-time weak measure solutions, finite-time aggregation and confinement for nonlocal interaction equations, 2011. to appear in the Duke Mathematical Journal.

[14] Hongjie Dong. The aggregation equation with power-law kernels: ill-posedness, mass concentration and similarity solutions, 2010. submitted.

[15] Jens Eggers and Marco A. Fontelos. The role of self-similarity in singularities of partial differential equations. *Nonlinearity*, 22(1):R1–R44, 2009.

[16] Darryl D. Holm and Vakhtang Putkaradze. Aggregation of finite-size particles with variable mobility. *Phys Rev Lett*, 95:226106, 2005.

[17] Darryl D. Holm and Vakhtang Putkaradze. Formation of clumps and patches in self-aggregation of finite-size particles. *Phys. D*, 220(2):183–196, 2006.

[18] Yanghong Huang. *Self-Similar Blowup Solutions of the Aggregation Equation*. PhD thesis, University of California Los Angeles, 2010. available online as UCLA CAM Report 10-66.

[19] Yanghong Huang and Andrea L. Bertozzi. Self-similar blowup solutions to an aggregation equation in R^n. *SIAM J. Appl. Math.*, 70(7):2582–2603, 2010.

[20] Yanghong Huang, Thomas Witelski, and Anrea Bertozzi. Anomalous exponents of self-similar blowup solution to an aggregation equation in odd dimensions, 2010. preprint.

[21] Thomas Laurent. Local and global existence for an aggregation equation. *Comm. Partial Differential Equations*, 32(10-12):1941–1964, 2007.

[22] Hailiang Li and Giuseppe Toscani. Long-time asymptotics of kinetic models of granular flows. *Arch. Ration. Mech. Anal.*, 172(3):407–428, 2004.

[23] Alexander Mogilner and Leah Edelstein-Keshet. A non-local model for a swarm. *J. Math. Biol.*, 38(6):534–570, 1999.

[24] Chad M. Topaz and Andrea L. Bertozzi. Swarming patterns in a two-dimensional kinematic model for biological groups. *SIAM J. Appl. Math.*, 65(1):152–174 (electronic), 2004.

[25] Chad M. Topaz, Andrea L. Bertozzi, and Mark A. Lewis. A nonlocal continuum model for biological aggregation. *Bull. Math. Biol.*, 68(7):1601–1623, 2006.

[26] Giuseppe Toscani. One-dimensional kinetic models of granular flows. *M2AN Math. Model. Numer. Anal.*, 34(6):1277–1291, 2000.

[27] Cédric Villani. *Topics in optimal transportation*, volume 58 of *Graduate Studies in Mathematics*. American Mathematical Society, Providence, RI, 2003.